

Sensor and Simulation Notes

Note 521

December 2006

Transmission/Reflection at a Dielectric Slab

Carl E. Baum
University of New Mexico
Department of Electrical and Computer Engineering
Albuquerque New Mexico 87131

Abstract

This paper explores and categorizes various techniques for making a dielectric interface between two media for single frequency application (such as the exit from a pyramidal horn).

This work was sponsored in part by the Air Force Office of Scientific Research.

1. Introduction

In the design of high-power electromagnetic radiators and the associated pulsed power, one often encounters the problem of transitioning electromagnetic waves between different media (e.g., air, vacuum, SF₆, oil). For fast pulses (or hypoband CW high frequencies) one is concerned about reflections at the interface between the two media. Often a solid dielectric is used to separate the two media. If there is a pressure differential across this barrier, one must use appropriately strong materials to withstand the force. At the same time one is sometimes concerned with the mass (and volume) associated with the dielectric interface.

Consistent with the above, one must also be concerned with the electromagnetic properties of the interface to avoid unwanted reflections and transmit the electromagnetic wave in an optimally useful form for its intended use farther along the wave-propagating system. This leads one to consider various types of interface designs for their relative advantages in the intended application.

2. Canonical Geometry: Dielectric Slab

Figure 2.1 shows the geometry. We have a dielectric slab of thickness d and relative permittivity.

$$\epsilon_r \equiv \frac{\epsilon_2}{\epsilon_1} \quad (2.1)$$

A plane wave is incident from the left with angle of incidence ψ_i giving

$$\begin{aligned} \vec{1}_i &= \cos(\psi_i) \vec{1}_z + \sin(\psi_i) \vec{1}_x \\ \vec{1}_r &= -\cos(\psi_i) \vec{1}_z + \sin(\psi_i) \vec{1}_x \text{ (reflected wave)} \end{aligned} \quad (2.2)$$

The transmitted wave (past $z = d$) is also characterized by ψ_t . Inside the slab there are two waves characterized by ψ_t with

$$\begin{aligned} \vec{1}_{r'} &= \cos(\psi_t) \vec{1}_z + \sin(\psi_t) \vec{1}_x \\ \vec{1}_{r''} &= -\cos(\psi_t) \vec{1}_z + \sin(\psi_t) \vec{1}_x \end{aligned} \quad (2.3)$$

We also need for outside the slab

$$\begin{aligned} \vec{1}_p &= -\sin(\psi_i) \vec{1}_z + \cos(\psi_i) \vec{1}_x \\ \vec{1}_{p0} &= \sin(\psi_i) \vec{1}_z + \cos(\psi_i) \vec{1}_x \end{aligned} \quad (2.4)$$

And for inside the slab

$$\begin{aligned} \vec{1}_{p'} &= -\sin(\psi_t) \vec{1}_z + \cos(\psi_i) \vec{1}_x \\ \vec{1}_{r'} &= \cos(\psi_t) \vec{1}_z + \sin(\psi_t) \vec{1}_x \\ \vec{1}_{p''} &= \sin(\psi_t) \vec{1}_z + \cos(\psi_t) \vec{1}_x \\ \vec{1}_{r''} &= -\cos(\psi_t) \vec{1}_z + \sin(\psi_t) \vec{1}_x \end{aligned} \quad (2.5)$$

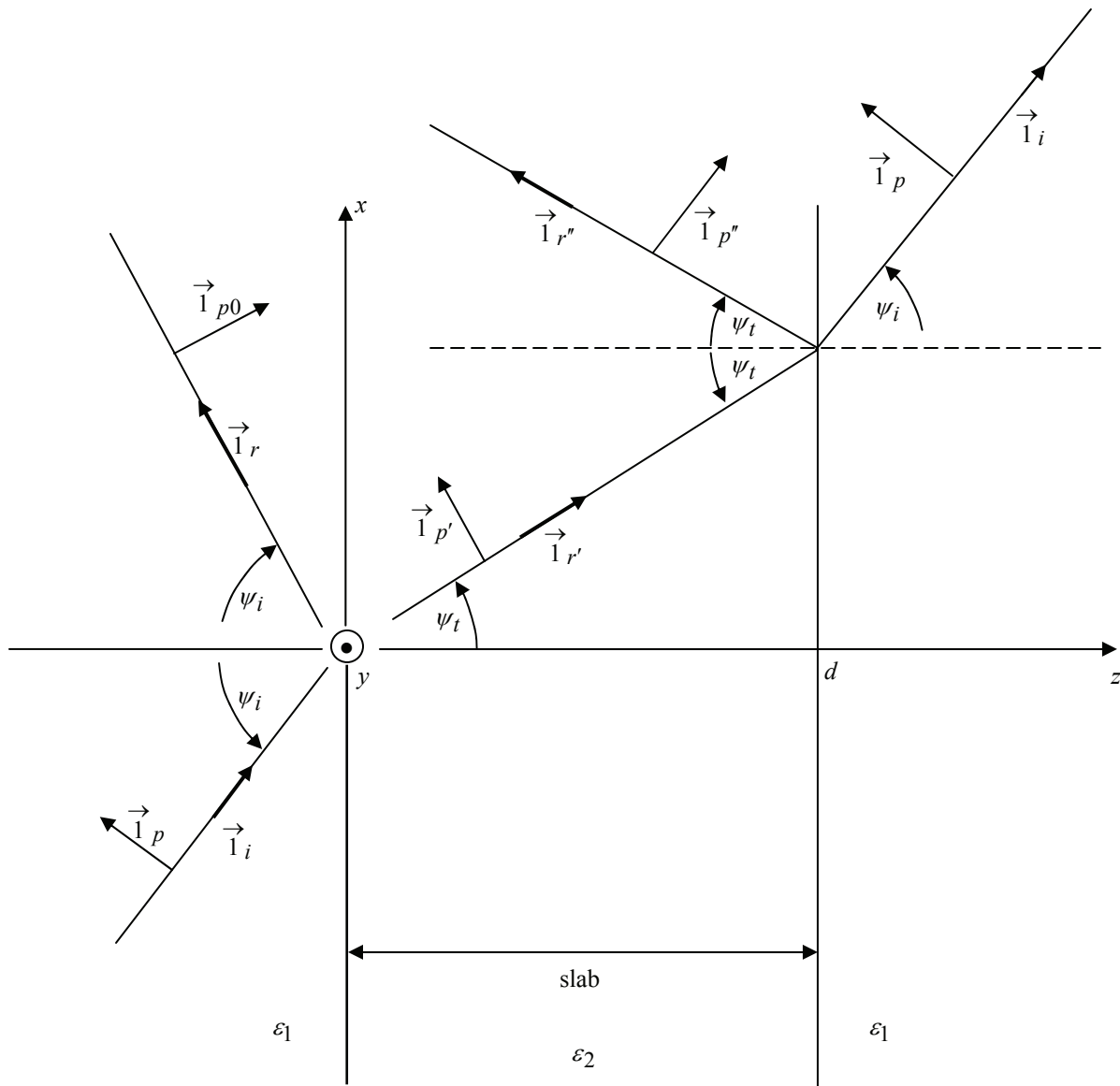


Fig. 2.1 Transmission Through and Reflection At a Dielectric Slab

These unit vectors are all parallel to the plane of incidence.

Matching phase speeds on the two boundaries implies

$$\begin{aligned}
 e^{-\gamma_1 \sin(\psi_i)x} &= e^{-\gamma_2 \sin(\psi_t)x} \\
 \gamma_1 &= \frac{s}{v_1}, \quad v_1 = [\mu\epsilon_1]^{-1/2} \\
 \gamma_2 &= \frac{s}{v_2}, \quad v_2 = [\mu\epsilon_2]^{-1/2} \\
 \epsilon_1^{1/2} \sin(\psi_i) &= \epsilon_2^{1/2} \sin(\psi_t) \\
 \sin(\psi_i) &= \epsilon_r^{1/2} \sin(\psi_t) \\
 s &= \Omega + j\omega \equiv \text{Laplace transform variable (two-sided) or complex frequency} \\
 \gamma &= jk \text{ for } s = j\omega \text{ (propagation constant)}
 \end{aligned} \tag{2.6}$$

The above applies to both polarizations. We also have

$$\begin{aligned}
 Z_1 &= \left[\frac{\mu}{\epsilon_1} \right]^{1/2}, \quad Z_2 = \left[\frac{\mu}{\epsilon_2} \right]^{1/2}, \quad \frac{Z_2}{Z_1} = \epsilon_r^{-1/2} \text{ (wave impedances)} \\
 \frac{\gamma_2}{\gamma_1} &= \epsilon_r^{1/2}
 \end{aligned} \tag{2.7}$$

2.1 E wave

This is specified by the electric field parallel to the plane of incidence, i.e., in the $\vec{1}_p$ direction in Fig. 2.1. The E (or TM) wave incident is

$$\vec{E}_e = E_0 \vec{1}_p e^{-\gamma_1 \vec{1}_i \cdot \vec{r}}, \quad \vec{H}_e = \frac{E_0}{Z_1} \vec{1}_y e^{-\gamma_1 \vec{1}_i \cdot \vec{r}} \tag{2.8}$$

The transmitted wave has

$$\vec{E}_t = T_e E_0 \vec{1}_p e^{-\gamma_1 \vec{1}_i \cdot \vec{r}}, \quad \vec{H}_t = T_e \frac{E_0}{Z_1} \vec{1}_y e^{-\gamma_1 \vec{1}_i \cdot \vec{r}} \tag{2.9}$$

The reflected wave has

$$\vec{E}_r = R_e E_0 \vec{1}_{p0} e^{-\gamma_1 \vec{1}_r \cdot \vec{r}}, \quad \vec{H}_r = -R_e \frac{E_0}{Z_1} \vec{1}_y e^{-\gamma_1 \vec{1}_r \cdot \vec{r}} \quad (2.10)$$

Inside the slab we have two waves given by

$$\begin{aligned} \vec{E}_{in} &= T_1 E_0 \vec{1}_{p'} e^{-\gamma_2 \vec{1}_{r'} \cdot \vec{r}} + T_2 E_0 \vec{1}_{p''} e^{-\gamma_1 \vec{1}_{r''} \cdot \vec{r}} \\ \vec{H}_{in} &= T_1 \frac{E_0}{Z_2} \vec{1}_y e^{-\gamma_2 \vec{1}_{r'} \cdot \vec{r}} - T_2 \frac{E_0}{Z_2} \vec{1}_y e^{-\gamma_2 \vec{1}_{r''} \cdot \vec{r}} \end{aligned} \quad (2.11)$$

2.1.1 Boundary conditions at $z = d$

For continuous tangential E we have

$$\begin{aligned} T_1 \cos(\psi_t) e^{-\gamma_2 d \cos(\psi_t)} + T_2 \cos(\psi_t) e^{\gamma_2 d \cos(\psi_t)} &= T_e \cos(\psi_i) e^{-\gamma_1 d \cos(\psi_i)} \\ \frac{\cos(\psi_t)}{\cos(\psi_i)} \left[T_1 e^{-\gamma_2 d \cos(\psi_t)} + T_2 e^{\gamma_2 d \cos(\psi_t)} \right] &= T_e e^{-\gamma_1 d \cos(\psi_i)} \end{aligned} \quad (2.12)$$

For continuous tangential H we have

$$\begin{aligned} \frac{T_1}{Z_2} e^{-\gamma_2 d \cos(\psi_t)} - \frac{T_2}{Z_2} e^{\gamma_2 d \cos(\psi_t)} &= \frac{T_e}{Z_1} e^{-\gamma_1 d \cos(\psi_i)} \\ \varepsilon_r^{1/2} \left[T_1 e^{-\gamma_2 d \cos(\psi_t)} - T_2 e^{\gamma_2 d \cos(\psi_t)} \right] &= T_e e^{-\gamma_1 d \cos(\psi_i)} \end{aligned} \quad (2.13)$$

Subtracting the two to eliminate T_e gives

$$\begin{aligned}
& \left[\frac{\cos(\psi_t)}{\cos(\psi_i)} - \varepsilon_r^{1/2} \right] T_1 e^{-\gamma_2 d \cos(\psi_t)} + \left[\frac{\cos(\psi_t)}{\cos(\psi_i)} + \varepsilon_r^{1/2} \right] T_2 e^{\gamma_2 d \cos(\psi_t)} \\
& \qquad \qquad \qquad = 0 \\
\frac{T_2}{T_1} &= - \frac{\frac{\cos(\psi_t)}{\cos(\psi_i)} - \varepsilon_r^{1/2}}{\frac{\cos(\psi_t)}{\cos(\psi_i)} + \varepsilon_r^{1/2}} e^{-2\gamma_2 d \cos(\psi_t)} \\
&= \frac{1 - \varepsilon_r^{-1/2} \frac{\cos(\psi_t)}{\cos(\psi_i)}}{1 + \varepsilon_r^{-1/2} \frac{\cos(\psi_t)}{\cos(\psi_i)}} e^{-2\gamma_2 d \cos(\psi_t)}
\end{aligned} \tag{2.14}$$

This gives an input impedance at $x = 0$ of

$$\begin{aligned}
Z_{in} &= \frac{E_{\tan}}{H_{\tan}} = \frac{\cos(\psi_t)[T_1 + T_2]}{\frac{1}{Z_2}[T_1 - T_2]} \\
&= Z_2 \cos(\psi_t) \frac{1 + \frac{T_2}{T_1}}{1 - \frac{T_2}{T_1}} \\
\frac{Z_{in}}{Z_1} &= \varepsilon_r^{-1/2} \cos(\psi_t) \frac{1 + \frac{T_2}{T_1}}{1 - \frac{T_2}{T_1}}
\end{aligned} \tag{2.15}$$

2.1.2 Boundary conditions at $z = 0$

Let us match tangential E and H to Z_{in} as

$$Z_{in} = \frac{\cos(\psi_i)[1 + R_e]}{Z_1^{-1}[1 - R_e]} \tag{2.16}$$

Solving for R_e

$$\begin{aligned}
R_e &= \frac{\frac{Z_{in}}{Z_1} - \cos(\psi_i)}{\frac{Z_{in}}{Z_1} + \cos(\psi_i)} \\
&= \frac{\varepsilon_r^{-1/2} \frac{\cos(\psi_t)}{\cos(\psi_i)} \left[1 + \frac{T_2}{T_1} \right] - \left[1 - \frac{T_2}{T_1} \right]}{\varepsilon_r^{-1/2} \frac{\cos(\psi_t)}{\cos(\psi_i)} \left[1 + \frac{T_2}{T_1} \right] + \left[1 - \frac{T_2}{T_1} \right]} \\
&= \frac{\left[\varepsilon_r^{-1/2} \frac{\cos(\psi_t)}{\cos(\psi_i)} - 1 \right] + \left[\varepsilon_r^{-1/2} \frac{\cos(\psi_t)}{\cos(\psi_i)} + 1 \right] \frac{T_2}{T_1}}{\left[\varepsilon_r^{-1/2} \frac{\cos(\psi_t)}{\cos(\psi_i)} + 1 \right] + \left[\varepsilon_r^{-1/2} \frac{\cos(\psi_t)}{\cos(\psi_i)} - 1 \right] \frac{T_2}{T_1}}
\end{aligned} \tag{2.17}$$

Combining with (2.14) gives

$$R_e = \frac{\left[\varepsilon_r^{-1} \frac{\cos^2(\psi_t)}{\cos^2(\psi_i)} - 1 \right] \left[1 - e^{-2\gamma_2 d \cos(\psi_t)} \right]}{\left[\varepsilon_r^{-1/2} \frac{\cos(\psi_t)}{\cos(\psi_i)} + 1 \right]^2 - \left[\varepsilon_r^{-1/2} \frac{\cos(\psi_t)}{\cos(\psi_i)} - 1 \right]^2 e^{-2\gamma_2 d \cos(\psi_t)}} \tag{2.18}$$

2.1.3 Brewster angle

For the special case of the Brewster angle both R_e and T_2 are zero. This implies from (2.14) and

(2.18)

$$\begin{aligned}
\varepsilon_r^{-1} \frac{\cos^2(\psi_t)}{\cos^2(\psi_i)} &= 1 \\
\varepsilon_r^{-1} \left[1 - \sin^2(\psi_t) \right] &= 1 - \sin^2(\psi_i) = \varepsilon_r^{-1} - \varepsilon_r^{-2} \sin^2(\psi_i) \\
\sin^2(\psi_i) &= \frac{\varepsilon_r}{\varepsilon_r + 1}, \quad \tan^2(\psi_i) = \varepsilon_r \\
\sin^2(\psi_t) &= \frac{1}{\varepsilon_r + 1}, \quad \tan^2(\psi_t) = \frac{1}{\varepsilon_r} \\
\psi_i + \psi_t &= \frac{\pi}{2}
\end{aligned} \tag{2.19}$$

2.1.4 Special frequencies

For zero reflected wave ($R_e = 0$) we can look at the numerator in (2.18). The first factor gives the Brewster angle. The second factor gives

$$\begin{aligned} e^{-2jK_2d \cos(\psi_t)} &= 1 \\ 2K_2d \cos(\psi_t) &= 0, 2\pi, 4\pi, \dots \end{aligned} \quad (2.20)$$

For a given ω and v_2 only certain thicknesses, multiples of a half wavelength in the slab (including dependence on ψ_t via ψ_i (2.6)), are appropriate.

Let us look for other special frequencies for which $R_e = 0$. Since the denominator of (2.18) is bounded (can't be ∞), that leaves the numerator. The two factors of the numerator can each be zero. The first gives the Brewster angle in (2.19). The second gives the special frequencies in (2.20). There are no more zeros, and therefore, no more special frequencies.

2.1.5 Thin slab

We can obtain a small reflection if $d \ll \lambda$. The slab can then be thought of as a membrane. For this purpose we expand

$$e^{-2\gamma_2d \cos(\psi_t)} = 1 - 2\gamma_2d \cos(\psi_t) + O([\gamma_2d]^2) \quad (2.21)$$

In (2.18) then we have (to first order)

$$\begin{aligned} R_e &= \frac{\left[\varepsilon_r^{-1} \frac{\cos^2(\psi_t)}{\cos^2(\psi_i)} - 1 \right] 2\gamma_2d \cos(\psi_t)}{4\varepsilon_r^{-1/2} \frac{\cos(\psi_t)}{\cos(\psi_i)}} \\ &= \frac{1}{2} \varepsilon_r^{1/2} \cos(\psi_i) \left[\varepsilon_r^{-1} \frac{\cos^2(\psi_t)}{\cos^2(\psi_i)} - 1 \right] \gamma_2d \\ &= -\frac{1}{2} \cos(\psi_i) \left[\varepsilon_r - \frac{\cos^2(\psi_t)}{\cos^2(\psi_i)} \right] \gamma_1d \\ &= -\frac{1}{2} \cos(\psi_i) \frac{\varepsilon_r - 1}{\varepsilon_r} \left[\varepsilon_r + 1 - \sec^2(\psi_i) \right] \gamma_1d \end{aligned} \quad (2.22)$$

For normal incidence this reduces to

$$R_e = -\frac{\epsilon_r - 1}{2} \gamma_1 d \quad (2.23)$$

which can be made quite small.

2.2 H wave

This is specified by the magnetic field parallel to the plane of incidence, i.e., in the $\vec{1}_p$ direction in Fig. 2.1. The H (or TE) wave incident is

$$\vec{E}_h = -E_0 \vec{1}_y e^{-\gamma_1 \vec{1}_i \cdot \vec{r}}, \quad \vec{H}_h = \frac{E_0}{Z_1} \vec{1}_p e^{-\gamma_1 \vec{1}_i \cdot \vec{r}} \quad (2.24)$$

The transmitted wave has

$$\vec{E}_t = -T_h E_0 \vec{1}_y e^{-\gamma_1 \vec{1}_i \cdot \vec{r}}, \quad \vec{H}_t = T_h \frac{E_0}{Z_1} \vec{1}_p e^{-\gamma_1 \vec{1}_i \cdot \vec{r}} \quad (2.25)$$

The reflected wave has

$$\vec{E}_r = R_h E_0 \vec{1}_y e^{-\gamma_1 \vec{1}_r \cdot \vec{r}}, \quad \vec{H}_r = R_h \frac{E_0}{Z_1} \vec{1}_p e^{-\gamma_1 \vec{1}_r \cdot \vec{r}} \quad (2.26)$$

Inside the slab the two waves are

$$\begin{aligned} \vec{E}_{in} &= -T_1 E_0 \vec{1}_y e^{-\gamma_2 \vec{1}_{r'} \cdot \vec{r}} + T_2 E_0 \vec{1}_y e^{\gamma_2 \vec{1}_{r''} \cdot \vec{r}} \\ \vec{H}_{in} &= T_1 \frac{E_0}{Z_2} \vec{1}_{p'} e^{-\gamma_2 \vec{1}_{r'} \cdot \vec{r}} + T_2 \frac{E_0}{Z_2} \vec{1}_{p''} e^{\gamma_2 \vec{1}_{r''} \cdot \vec{r}} \end{aligned} \quad (2.27)$$

2.2.1 Boundary conditions at $z = d$

Continuous tangential E gives

$$-T_1 e^{-\gamma_2 d \cos(\psi_t)} + T_2 e^{\gamma_2 d \cos(\psi_t)} = -T_h e^{-\gamma_1 d \cos(\psi_i)} \quad (2.28)$$

Continuous tangential H gives

$$\begin{aligned} \frac{T_1}{Z_2} \cos(\psi_t) e^{-\gamma_2 d \cos(\psi_t)} + \frac{T_2}{Z_2} \cos(\psi_t) e^{\gamma_2 d \cos(\psi_t)} &= \frac{T_h}{Z_1} \cos(\psi_i) e^{-\gamma_1 d \cos(\psi_i)} \\ \varepsilon_r^{1/2} \frac{\cos(\psi_t)}{\cos(\psi_i)} \left[T_1 e^{-\gamma_2 d \cos(\psi_t)} + T_2 e^{\gamma_2 d \cos(\psi_t)} \right] &= T_h e^{-\gamma_1 d \cos(\psi_i)} \end{aligned} \quad (2.29)$$

Add the two to eliminate T_h giving

$$\begin{aligned} \left[\varepsilon_r^{1/2} \frac{\cos(\psi_t)}{\cos(\psi_i)} - 1 \right] T_1 e^{-\gamma_2 d \cos(\psi_t)} + \left[\varepsilon_r^{1/2} \frac{\cos(\psi_t)}{\cos(\psi_i)} + 1 \right] T_2 e^{\gamma_2 d \cos(\psi_t)} \\ \frac{T_2}{T_1} = - \frac{\varepsilon_r^{1/2} \cos(\psi_t) - 1}{\varepsilon_r^{1/2} \cos(\psi_i) + 1} e^{-2\gamma_2 d \cos(\psi_t)} \end{aligned} \quad (2.30)$$

The input impedance at $x = 0$ is

$$\begin{aligned} Z_{in} &= \frac{E_{\tan}}{H_{\tan}} = \frac{-T_1 + T_2}{\frac{1}{Z_2} [T_1 + T_2] \cos(\psi_t)} \\ &= - \frac{Z_2}{\cos(\psi_t)} \frac{1 - \frac{T_2}{T_1}}{1 + \frac{T_2}{T_1}} \\ \frac{Z_{in}}{Z_1} &= - \frac{1}{\varepsilon_r^{1/2} \cos(\psi_t)} \frac{1 - \frac{T_2}{T_1}}{1 + \frac{T_2}{T_1}} \end{aligned} \quad (2.31)$$

2.2.2 Boundary conditions at $z = 0$

Matching tangential E and H at Z_{in} as

$$Z_{in} = \frac{-1 + R_h}{\frac{\cos(\psi_i)}{Z_i} [1 + R_h]} = - \frac{Z_1}{\cos(\psi_i)} \frac{1 - R_h}{1 + R_h} \quad (2.32)$$

This gives

$$\begin{aligned}
R_h &= \frac{1 + \cos(\psi_i) \frac{Z_{in}}{Z_1}}{1 - \cos(\psi_i) \frac{Z_{in}}{Z_1}} \\
&= \frac{\varepsilon_r^{1/2} \frac{\cos(\psi_t)}{\cos(\psi_i)} \left[1 + \frac{T_2}{T_1} \right] - \left[1 - \frac{T_2}{T_1} \right]}{\varepsilon_r^{1/2} \frac{\cos(\psi_t)}{\cos(\psi_i)} \left[1 + \frac{T_2}{T_1} \right] + \left[1 - \frac{T_2}{T_1} \right]} \\
&= \frac{\left[\varepsilon_r^{1/2} \frac{\cos(\psi_t)}{\cos(\psi_i)} - 1 \right] + \left[\varepsilon_r^{1/2} \frac{\cos(\psi_t)}{\cos(\psi_i)} + 1 \right] \frac{T_2}{T_1}}{\left[\varepsilon_r^{1/2} \frac{\cos(\psi_t)}{\cos(\psi_i)} + 1 \right] + \left[\varepsilon_r^{1/2} \frac{\cos(\psi_t)}{\cos(\psi_i)} - 1 \right] \frac{T_2}{T_1}} \tag{2.33}
\end{aligned}$$

Combining with (2.30) gives

$$R_h = \frac{\left[\varepsilon_r^{1/2} \frac{\cos(\psi_t)}{\cos(\psi_i)} - 1 \right] \left[1 - e^{-2\gamma_2 d \cos(\psi_t)} \right]}{\left[\varepsilon_r^{1/2} \frac{\cos(\psi_t)}{\cos(\psi_i)} + 1 \right] - \left[\varepsilon_r^{1/2} \frac{\cos(\psi_t)}{\cos(\psi_i)} - 1 \right]^{1/2} e^{-2\gamma_2 d \cos(\psi_t)}} \tag{2.34}$$

2.2.4 Special frequencies

There are two factors in the numerator of (2.34) in which one can look for zeros. There is no real ψ_i to make the first factor zero (no Brewster angle). The second factor has zeros at

$$2\gamma_2 d \cos(\psi_t) = 0, 2\pi, 4\pi, \dots \tag{2.35}$$

the same as (2.20) for the E-wave case.

This exhausts the case of reflection zero (total power transmission).

2.2.4 Thin slab

Again we can have a small reflection if $d \ll \lambda$. Expand as in (2.21), giving to first order

Editor's Note: *Please refer to last page of this document for comments by Duixian Liu, PhD*

$$\begin{aligned}
R_h &= \frac{\left[\varepsilon_r \frac{\cos^2(\psi_t)}{\cos^2(\psi_i)} - 1 \right] 2\gamma_2 d \cos(\psi_t)}{4\varepsilon_r^{1/2} \frac{\cos(\psi_t)}{\cos(\psi_i)}} \\
&= \frac{1}{2} \varepsilon_r^{-1/2} \cos(\psi_i) \left[\varepsilon_r \frac{\cos^2(\psi_t)}{\cos^2(\psi_i)} - 1 \right] \gamma_2 d \\
&= \frac{1}{2} \cos(\psi_i) \left[\varepsilon_r \frac{\cos^2(\psi_t)}{\cos^2(\psi_i)} - 1 \right] \gamma_1 d \\
&= -\frac{1}{2} \cos(\psi_i) \frac{\varepsilon_r - 1}{-\varepsilon_r} \left[[\varepsilon_r + 1] \sec^2(\psi_i) - 1 \right] \gamma_1 d
\end{aligned} \tag{2.36}$$

For normal incidence this reduces to the same formula as in (2.23).

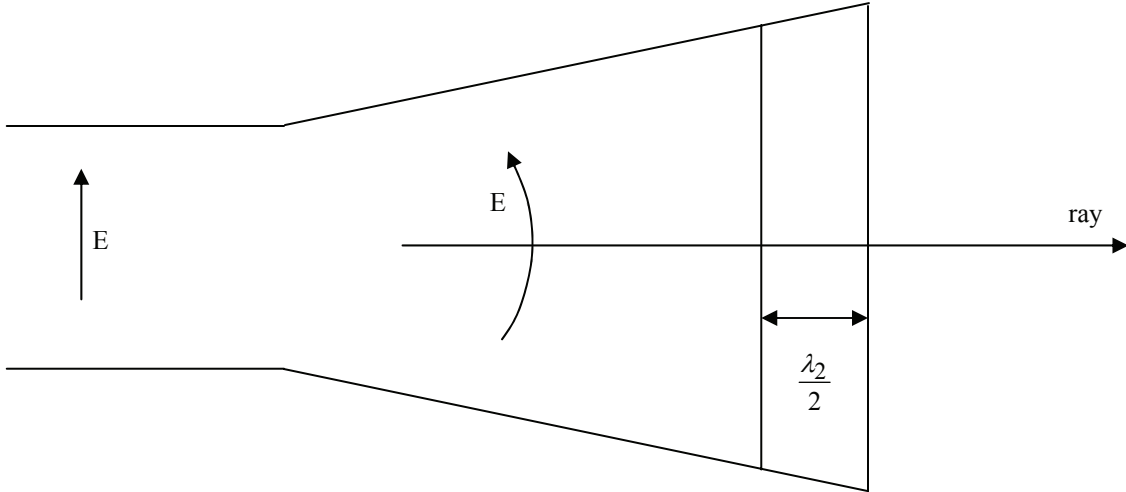
3. Slab for $H_{1,0}$ Horn Mode

Utilizing the Brewster-angle technique (Section 2.1.3), various applications of this for TEM plane waves are discussed in [2, 3], applying to transient pulses as well as single frequency (hypoband) applications. Another case of almost-TEM waves concerns radiation from a pyramidal horn as in Fig. 3.1. The $H_{1,0}$ mode of a standard rectangular waveguide has a longitudinal component of the E field. As the wave expands in a pyramidal horn we can think of this as a waveguide *way* above cutoff, for which this longitudinal component can be quite small. So we can think of this wave near the horn exit as almost TEM. Note, however, the planar characteristic is only approximate, it being more accurately described as spherical. The orientation of both fields varies to some degree as one moves across the horn exit.

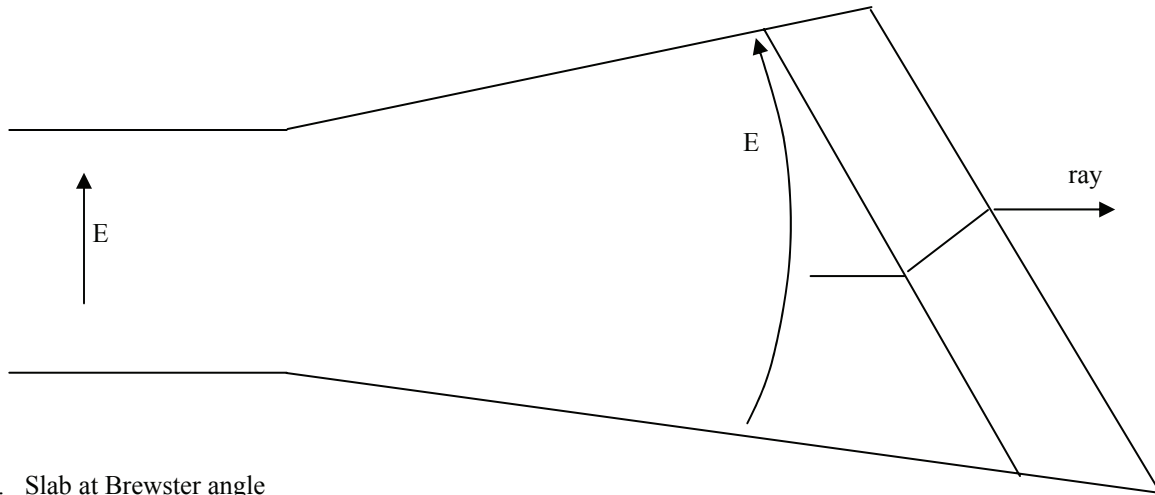
Figure 3.1A shows the case of a $\lambda_2/2$ thick slab for approximate normal incidence at the horn exit. The function of this slab is to separate two media such as vacuum and gas (air, SF_6 , etc.). In such an application, at lower microwave frequencies, the horn exit can be large implying a large force exerted by the gas on the slab. The large slab can also be quite massive. In line with the frequency dependence of the optimum thickness in (2.20) and (2.35) one could also taper the thickness as one moves away from the center of the slab.

An alternative approach in Fig. 3.1B utilizes the Brewster angle in Section 2.1.3. This sloping of the slab at the horn exit can increase the length of the horn and size (area) of the slab, thereby increasing the force to be withstood. However, the use of the Brewster angle removes the electromagnetic requirement on slab thickness. Since the orientations of the fields vary to some degree over the horn exit, a flat slab will have a “perfect” match at one point (the center), unless one curves the slab. Of course, one can try to doubly remove the reflection by the simultaneous use of the Brewster-angle and half-wavelength thickness conditions.

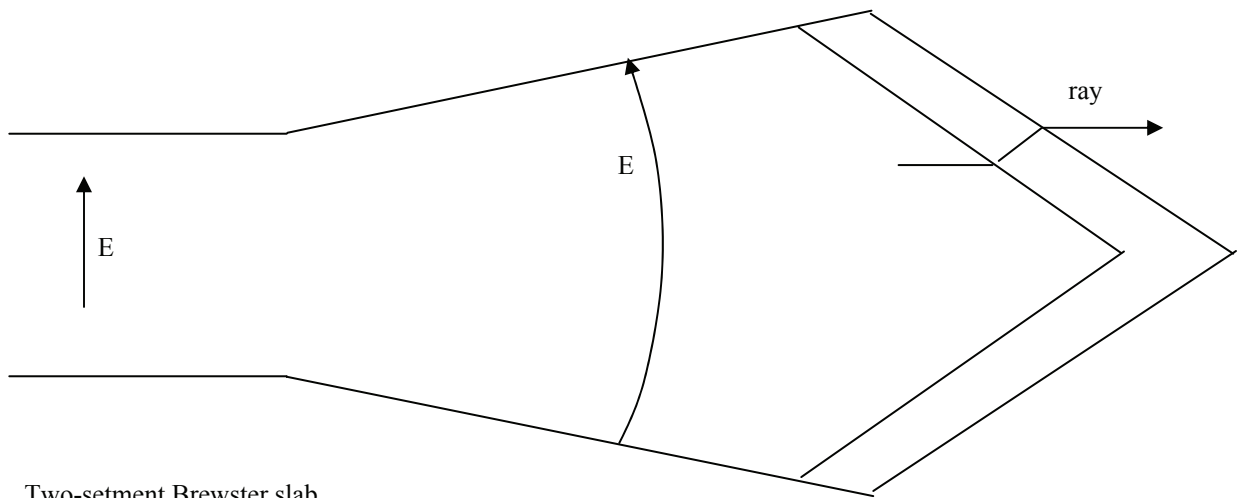
One way to reduce the size of a Brewster slab is illustrated in Fig. 3.1C. Here the slab is made in two segments with opposite slopes, but joined together in the middle. The gas pressure can aid in forcing the two parts together. Now the optimal choice for the Brewster angle is based, not on the joining center, but on positions away from the center to obtain a better average value for the angle over the two-segment slab. There is, however, an electromagnetic perturbation at the joining center. Again the Brewster technique can be combined with the half-wavelength technique.



A. Slab at normal incidence



B. Slab at Brewster angle



C. Two-setment Brewster slab

Fig. 3.1 Slab At Horn Exit

4. Metal Reinforced Diaphragm for $H_{1,0}$ Horn Mode

As discussed in [1, 4] another approach utilizes a thin dielectric slab, i.e., a diaphragm, at the horn exit as illustrated in Fig. 4.1. In this case we have a very small reflection coefficient for “all” angles of incidence as in (2.22) and (2.36). This raises the question of withstanding a large force across the horn exit. This is solved by the use of metal slats perpendicular to the incident electric field. See the discussion in [1, 4] for some variations on this theme. For example, the doubly sloped form in Fig. 3.1C can also use this technique.

In this case one should be careful that the slat lengths are not an integer number of half wavelengths in length. Such resonances can also be avoided by tapering the slats to give added inductance or capacitance at appropriate positions. If one operates the horn at two or more separated frequencies, the nonresonant condition will need to be satisfied at all these frequencies.

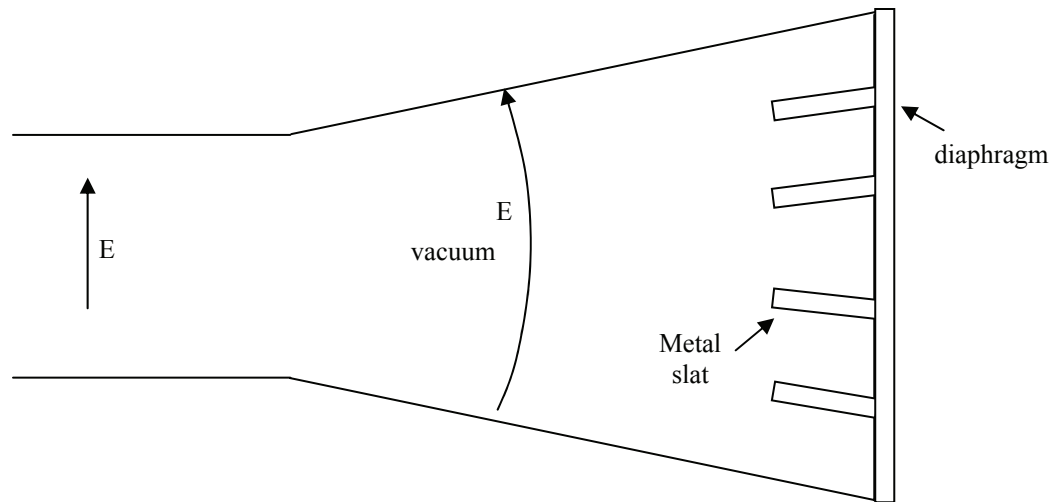


Fig. 4.1 Reinforced Diaphragm

5. Concluding Remarks

So we now have several possible techniques for transitioning electromagnetic waves at single frequencies through a dielectric interface with only small reflection (i.e., near unity transmission). These include the Brewster-angle phenomenon, half-wavelength thickness, and thin reinforced diaphragm. Within each of these categories there are various optional shapes for the interface at a pyramidal-horn exit.

References

1. C. E. Baum, "Some Features of Waveguide/Horn Design", Sensor and Simulation Note 314, November 1988; ch. 11.3, pp. 480-497, in H. Kikuchi (ed.), *Environmental and Space Electromagnetics*, Springer-Verlag, 1991.
2. C. E. Baum, "Wedge Dielectric Lenses for TEM Waves Between Parallel Plates", Sensor and Simulation Note 332, September 1991.
3. C. E. Baum, "Brewster-Angle Interface Between Flat-Plate Conical Transmission Lines", Sensor and Simulation Note 389, November 1995.
4. C. E. Baum, "High-Power Scanning Waveguide Array", Sensor and Simulation Note 459, September 2001.

Many thanks to Duixian Liu, PhD. who wrote to us on May 21, 2021 with the following comments:

On page 12 of the the Note 521, eq (2.34) has typos in several locations. It seems the error for abs(Rh) is small for my calculations, however, the Error for Th based on Rh is huge.

Here is my corrected expression for eq (2.34). (at the bottom of the picture)

Also, the ratio T2/T1 in eq (2.30) has a typo: The angle PSIi should be PSI t on the denominator.

Also the first vector expression in eq (2.5) has a typo: The angle PSIi should be PSI t .

This is a very important Note. So correcting the typos will be very helpful.

Thanks.

Duixian Liu, PhD., Fellow of IEEE

Master Inventor
 Research Staff Member
 Wireless System Design & Packaging
 IBM Thomas J. Watson Research Center
 1101 Kitchawan Rd, Yorktown Heights, NY 10598
 Tel: 914-945-1278 Fax: 914-945-4219
 Email: duixian@us.ibm.com

